Title
Investigation of potential dragdown/uplift effects on energy piles

Authors
McCartney, John S
Murphy, Kyle D

Publication Date
2017-06-01

DOI
10.1016/j.gete.2017.03.001

Peer reviewed

Manuscript Details

Manuscript number	GETE_2016_23
Title	Investigation of Potential Dragdown/Uplift Effects on Energy Piles
Article type	Research Paper

Abstract

This study focuses on the interpretation of axial strains in a pair of full-scale energy piles beneath an 8-story building measured over the course of five years of geothermal heat pump operation. Although the cyclic temperature changes imposed upon the energy piles are consistent during each of the years of operation, the axial strains at different depths appear to show diverging trends. Evaluation of the profiles of thermal axial strain under different instances of extreme heating and cooling in each year of operation indicates that predominantly contractile strains are being superimposed atop the thermo-elastic expansion and contraction of the piles, especially near the toe of the piles. An evaluation of the trends in mobilized coefficient of thermal expansion during different heating and cooling cycles indicates that the superimposed contractile strains on the pile are not affecting the thermo-elastic expansion and contraction of the energy piles. Accordingly, the superimposed contractile strains were determined to be due to the effects of dragdown or uplift of the surrounding soil on the piles. The observed dragdown or uplift may be caused by thermal effects on the subsurface surrounding the piles or long-term mechanical compression of the subsurface under the applied building load, and deserve further study using more advanced analyses.

Keywords	Energy piles, cyclic effects, dragdown, uplift

Corresponding Author	John McCartney
Order of Authors	John McCartney, Kyle Murphy

Submission Files Included in this PDF

File Name [File Type]

2017-02-27 - GETE - McCartney and Murphy - Cover Letter.pdf [Cover Letter]

Author Questionnaire.docx [Author Agreement]

2017-02-27 - GETE - McCartney and Murphy - Response to Comments.docx [Response to Reviewers]

2017-02-27 - GETE - McCartney and Murphy - Manuscript.docx [Manuscript File]

Figure 1.tif [Figure]

Figure 2.tif [Figure]

Figure 3.tif [Figure]

FIgure 4.tif [Figure]

Figure 5.tif [Figure]

Figure 6.tif [Figure]

Figure 7.tif [Figure]

Figure 8.tif [Figure]

Figure 9.tif [Figure]

Highlights.docx [Highlights]

To view all the submission files, including those not included in the PDF, click on the manuscript title on your EVISE Homepage, then click 'Download zip file'.

Title: Investigation of Potential Dragdown/Uplift Effects on Energy Piles

Authors

John S. McCartney, Ph.D., P.E. (Corresponding Author)
Associate Professor
University of California San Diego
Department of Structural Engineering
9500 Gilman Drive
La Jolla, CA 92093-0085
Phone: (+1)858-534-9630
Email: mccartney@ucsd.edu

Kyle D. Murphy, M.S.
Engineer
Shannon & Wilson, Inc.
1321 Bannock St
Denver, CO 80204
Email: kdm@shanwil.com

Abstract

This study focuses on the interpretation of axial strains in a pair of full-scale energy piles beneath an 8-story building measured over the course of five years of geothermal heat pump operation. Although the cyclic temperature changes imposed upon the energy piles are consistent during each of the years of operation, the axial strains at different depths appear to show diverging trends. Evaluation of the profiles of thermal axial strain under different instances of extreme heating and cooling in each year of operation indicates that predominantly contractile strains are being superimposed atop the thermo-elastic expansion and contraction of the piles, especially near the toe of the piles. An evaluation of the trends in mobilized coefficient of thermal expansion during different heating and cooling cycles indicates that the superimposed contractile strains on the pile are not affecting the thermo-elastic expansion and contraction of the energy piles. Accordingly, the superimposed contractile strains were determined to be due to the effects of dragdown or uplift of the surrounding soil on the piles. The observed dragdown or uplift may be caused by thermal effects on the subsurface surrounding the piles or long-term mechanical compression of the subsurface under the applied building load, and deserve further study using more advanced analyses.

Introduction

Evaluation of instrumented energy piles in a field setting is the only way to fully consider the effects of installation, actual construction materials, subsurface stratigraphy, and restraints at the head and toe of the pile on the thermo-mechanical strains, stresses, and displacements induced by heating and cooling. Due to this fact, several field scale tests on instrumented energy piles have been performed that involved monotonic heating or cooling (Laloui et al. 2006; Bourne-Webb et al. 2009; Amatya et al. 2012; Sutman et al. 2014; Wang et al. 2014; Akrouch et al. 2015; Murphy et al. 2015). The details of these experiments have been summarized in detail by Olgun and McCartney (2015). Although very useful in interpreting soil-structure interaction phenomena in energy piles, one issue with monotonic heating or cooling tests is that time dependent effects that impact either the capacity of the energy pile such as setup or the stress distribution in the energy pile such as dragdown or uplift cannot be easily considered. These time-dependent effects are complex to analyze and predict even for conventional piles (Asakawa 1959; Bjerrum et al. 1969; Fellenius 1972; Budge et al. 2015), and may be more complex for energy piles in that temperature changes of the energy pile may affect the properties or cause volume changes of the surrounding subsurface (Laloui et al. 2015), lead to creep effects (Akrouch et al. 2015), or cause ratcheting effects in heavily-loaded piles undergoing cyclic heating and cooling (Suryatriastuti et al. 2013; Pasten and Santamarina 2014; Saggu and Chakraborty 2015; Di Donna et al. 2015). Although time-dependent effects can be assessed through long-term monitoring of embedded instrumentation in energy piles, fewer studies have been performed to assess the thermo-mechanical behavior of energy piles during long-term heating and cooling of energy piles associated with to operation of a geothermal heat pump used for building space conditioning (Brandl 1998; McCartney and Murphy 2012; Murphy and McCartney 2015). This paper revisits the case history described by Murphy and McCartney (2015) with new instrumentation data to assess the potential effects of dragdown or uplift caused by thermal or mechanical effects on the interpretation of the thermo-mechanical behavior of two energy piles installed at the site.

Brief Review of the Case History Details

McCartney and Murphy (2012) and Murphy and McCartney (2015) provide detailed information about two full-scale energy piles, referred to as Energy Pile A and Energy Pile B in this paper, constructed beneath an 8-story building in Denver, Colorado, USA. The site stratigraphy consists of urban fill atop a sandy gravel layer atop weathered claystone bedrock from the Denver Formation (locally referred to as Denver Blue Shale). The thicknesses of the soil layers along with measurements from in-situ site investigation tests are shown in Figure 1. Energy Pile A was installed under an interior building column, and has a depth of 14.8 m and a diameter of 0.91 m, while Energy Pile B was installed under an exterior building wall, and has a depth of 13.4 m and a diameter of 0.91 m. Both energy piles serve as end-bearing elements in the claystone, and were designed to carry vertical loads of 3.84 and 3.65 MN, respectively. Each shaft contains a full-length reinforcing cage that is 0.76 m in diameter with nine #7 vertical reinforcing bars tied to #3 lateral reinforcing hoops spaced 0.36 m on center. A reinforced concrete slab-on-grade with a thickness of 150 mm was cast at grade level and connected to the energy piles to provide a stiff upper boundary condition, which is important for understanding the potential thermal restraint (Goode and McCartney 2015). Energy Pile A includes three loops of polyethylene tubing having an inside diameter of 44 mm installed within the reinforcing cage, while Energy Pile B includes four loops of the same tubing. The energy piles were installed using a 10 m-long temporary casing through the urban fill and sandy gravel overburden and embedded into the claystone layer. Six concrete embedment vibrating wire strain gages (Model 52640299 from Slope Indicator of Mukilteo, WA) and co-located thermistors were incorporated into each energy pile at the depths shown in Figure 1. The vibrating wire strain gages were oriented longitudinally parallel to the axis of the energy pile and were attached to the lateral reinforcing hoops. One of the vibrating wire strain gages at a depth of 3.2 m in Energy Pile A was damaged during installation, but all of the other sensors were functional over the duration of this project (including the thermistor at a depth of 3.2 m in Energy Pile A). Over the five years of monitoring, the different data acquisition systems malfunctioned for short intervals due to different issues, including battery power loss, programming issues, and memory issues. Nonetheless, sufficient data is available to understand the long-term behavior of the energy piles. More details of the site, the conventional geothermal system, and the drilled shaft installation process are provided in McCartney and Murphy (2012) and Murphy and McCartney (2015).

Updated Time Series of Temperature and Strain

Time series of the temperatures of the heat exchanger fluids entering and exiting Energy Piles A and B are shown in Figure 2. Although the focus of this paper is on the thermo-mechanical response of the energy pile, these fluid temperatures are an important boundary condition for the energy piles, with a temperature ranging from 7 to 37 °C based on the heating and cooling demands of the heat pumps in the building. A discussion on the heat transfer that can be estimated using the information in this figure can be found in Murphy and McCartney (2015), and no different conclusions on this topic are drawn in this study from the updated time series. The concrete temperature at different depths in Energy Piles A and B are shown in Figures 3(a) and 3(b), respectively, and the corresponding changes in concrete temperature in Energy Piles A and B with respect to the initial condition corresponding to the start of heat pump operation are shown in Figure 3(c) and 3(d), respectively. The energy pile temperatures follow the same trends as the heat exchanger fluids, and it can be observed that the changes in pile temperature are relatively constant with depth in the energy pile. The temperatures at the toe of the energy piles were not measured, although the heat exchanger tubing extended throughout the length of the reinforcing cages. The magnitude of the extreme changes in temperature during heating and cooling are approximately the same in each year of operation.

The thermal axial strains were calculated using the approach described in Murphy and McCartney (2015), with the initial temperature on December 29, 2011 used as the reference point for changes in pile temperature, and are shown in Figures 3(e) and 3(f) for Energy Piles A and B, respectively. Because the strains in these figures were zeroed after all mechanical loading was applied (i.e., after the building was constructed and in operation), they should ideally only reflect the changes in axial strain in the pile due to temperature fluctuations. However, phenomena such as dragdown and uplift occur over long periods of time and may be superimposed atop these axial strains, which may complicate the interpretation of these values. Despite the fact that the concrete temperatures are within the same range on each year of operation, the thermal axial strains appear to diverge over time. This indicates that a temporal process is superimposed atop the thermo-elastic expansion and contraction of the energy piles. Further, Murphy and McCartney (2015) inspected the magnitudes of thermal axial strain and found that during extreme heating or cooling the thermal axial strains in both piles may be greater than those associated with free expansion of the reinforced concrete calculated using the temperature measured at the location of the strain gage. This conclusion is further exacerbated in the updated strain data measured since this previous study was published.

One hypothesis provided by Murphy and McCartney (2015) for the greater magnitude of thermal axial strains during these extreme heating and cooling events is that the strains in the energy pile are likely governed by the average temperature of the pile rather than the local temperature measured at the strain gage location, a topic that was also confirmed in numerical studies by Caulk et al. (2016) and Abdelaziz and Ozudogru (2016). A comparison between the average pile temperature and the outlet fluid temperature is shown in Figure 4, and a difference of up to 6 °C is observed in the summer months during pile heating, but less of a difference is noted in the winter months. Although use of the average pile temperature in the interpretation of the thermo-mechanical response of the energy piles may be more accurate than the use of the local temperatures, the changes in average pile temperature are still not sufficient to justify the inconsistencies in the measured thermal axial strain values with the theoretical thermal axial strains associated with free-expansion conditions. Further, the trends in the average pile temperature cannot be used to explain the temporal divergence of the thermal axial strain values over time observed in both energy piles. Sufficient information is not available from the site to tell if this temporal process is due to the temperature changes associated with the energy pile operation or other effects expected in constructing conventional piles in this area and the application of the building load. However, it is possible to isolate this temporal effect from the expected thermal expansion and contraction of the energy pile by evaluating profiles of axial strain in the energy pile at different moments of time that have the same changes in concrete temperature.

Thermal Expansion Evaluation

Although it is clear that there is a temporal effect superimposed atop the thermal axial strain time series in Figure 3, it is not clear if this temporal effect is changing the thermal expansion and contraction of the energy pile. For example, the temporal effect could lead to softening if it is leading to soil-pile displacements in the same direction as the pile movement during heating or cooling. In this case, softening would lead to less restraint of the energy pile and greater constrained expansion and contraction during heating or cooling, respectively. On the other hand, it is also possible this temporal effect could lead to densification of the subsurface surrounding the energy pile, leading to greater restraint. In order to investigate the thermal expansion and contraction of the energy pile over time, the average mobilized coefficient of thermal expansion can be calculated from the plots of the thermal axial strain versus temperature shown in Figures 5(a) and 5(b) for Energy Piles A and B, respectively. These plots reflect the temporal effect observed in Figure 3 in the form of a downward shift in some of the thermal axial strains with annual cycles. The average mobilized coefficients of thermal expansion at each depth in the energy piles were calculated as the average slope of the thermal axial strain data for each heating or cooling season during the four years (the data collected was insufficient to calculate the average slopes in 2016). The average mobilized coefficients of thermal expansion versus depth for Energy Piles A and B are shown in Figures 5(c) and 5(d), respectively. The dates given in the figure are the points of reversal at the end of each heating or cooling season. Assuming that the reinforced concrete has a coefficient of thermal expansion in unconstrained (free) conditions α_{free} of -13 $\mu\varepsilon$/°C used by Murphy and McCartney (2015), the difference between the mobilized value and the unconstrained value represents the restraint provided by the subsurface on the pile to thermal expansion and contraction. The fact that all of the mobilized coefficients of thermal expansion are less than -13 $\mu\varepsilon$/°C indicates that, on average, the energy piles are expanding and contracting less than if they were unconstrained. An interesting observation from this figure is that although there are variations in the profiles with each heating and cooling season, the variations do not seem to show a temporal effect. In fact, the greatest differences in the profiles of mobilized coefficients of thermal expansion are those for the first heating and cooling seasons. This observation indicates that the thermal expansion and contraction of the energy pile are not significantly affected by the temporal effect observed in the time series in Figures 3(e) and 3(f), and that the temporal effect is occurring mostly as an isolated phenomenon from the thermo-elastic expansion and contraction of the energy piles.

Thermal Dragdown/Uplift Evaluation

Because the thermo-elastic response of the energy piles is expected to be independent from the temporal effect observed in Figures 3(e) and 3(f), the approach proposed to study the potential impact of the temporal process is to compare the thermal axial strain profiles in the energy piles under extreme heating and cooling scenarios encountered at different moments in time during the five years of operation. First, different moments in time were identified where the energy pile experienced a given average change in temperature with depth during extreme heating and extreme cooling, as shown in Figures 6(a) and 6(b), respectively, for Energy Pile A, and in Figures 7(a) and 7(b), respectively, for Energy Pile B. The markers in these figures were selected so that they are open when the pile was experiencing a heating season and black when the pile was experiencing a cooling season. In all cases, the temperature was uniform with depth, and it is fair to say that the pile had the same temperature profile in each of the cases studied. The thermal axial strains during extreme heating and cooling corresponding to these temperature profiles are shown in Figures 6(c) and 6(d), respectively, for Energy Pile A, and in Figures 7(c) and 7(d), respectively, for Energy Pile B. The first observation that can be drawn from these figures is that the first instances of extreme heating (February 2012) and extreme cooling (July 2012) of the energy piles led to purely expansive and purely contractive strains, respectively. This is as expected, because when a pile is heated it should expand thermo-elastically. The amount of expansion may vary with depth depending on the restraints provided by the subsurface and overlying building, but it is not possible for the concrete to contract during heating. The next observation that can be drawn from these profiles is that successively larger contractile (positive) strains are observed over time near the toe of both piles for both the cases of extreme heating and extreme cooling. This again confirms that a temporal process is superimposed atop the thermal expansion and contraction of the energy piles.

To estimate the amount of axial strain induced in the energy piles due to the temporal process, the difference between the profiles from the first extreme heating event and the extreme heating event in 2015 are shown in Figures 8(a) and 8(b) for Energy Piles A and B, respectively. For both piles, a contractile strain profile was observed (with the exception of one depth in Energy Pile B), with greater values of contractile strain near the toe of the pile. Next, the contractile strains were subtracted from the strains observed during extreme cooling, as shown in Figures 8(c) and 8(d) for Energy Piles A and B, respectively. This approach is not exactly correct, as it is expected that the temporal process may have continued to occur between the instances in time associated with extreme heating and extreme cooling, but it permits an approximate evaluation of this hypothesis. In both energy piles, the "corrected" thermal axial strain profile obtained by subtracting the contractile strain profile leads to a thermal axial strain profile that is close to that observed on the first extreme cooling event. Although approximate, this analysis indicates that the temporal effect is leading to a predominantly contractile strain profile that is evolving over time and is superimposed atop the thermal axial strain profiles during extreme heating and cooling.

It should be noted that the predominantly contractile strains observed in Figure 8 could be due to either downdrag or uplift. In the case of downdrag, the overlying fill and sandy gravel layers are settling over time, imposing downward frictional forces on the energy pile that react against the end bearing resistance similar to the observations by Bjerrum et al. (1969). In the case of uplift, the claystone may be hydrating due to exposure to water facilitated by the drilled shaft installation. This may lead to an upward swelling of the claystone, imposing upward frictional forces on the energy pile that react against the weight of the pile and overlying building. It is also possible that the claystone may be experiencing drying and associated shrinkage due to the exposure to elevated temperatures, similar to the thermally induced water flow observed in unsaturated Bonny silt during monotonic heating experiments on energy piles by Goode and McCartney (2015). However, thermally induced water flow in claystone is likely very slow and would require a monotonic thermal gradient that is not present in the operation of the energy piles evaluated in this study. Nonetheless, the greater contractile strains near the toe of the pile indicate that dragdown is the more likely cause of the temporal effects (so dragdown in used to explain the phenomena in the figures for simplicity). More advanced simulations are needed to confirm this hypothesis.

Axial Stress Evaluation

Now that the dragdown axial strains have been isolated from the thermal axial strains, it is possible to convert the thermal axial strains in the energy pile into thermal axial stresses. The thermal axial stresses σ_{aT} can be calculated from the thermal axial strains ε_{aT} as follows:

$$\sigma_{aT} = E(\varepsilon_{aT} - \alpha_{free}\Delta T) \qquad (1)$$

where E is the Young's modulus and ΔT is the change in temperature at a given depth (which should ideally be the average change in temperature across the cross-sectional area of the pile, but is assumed to be the change in temperature at the location of the strain gage for simplicity). The isolated dragdown axial strains ε_{aD} can be converted to dragdown axial stresses σ_{aD} using Hooke's law as follows:

$$\sigma_{aD} = E\varepsilon_{aD} \qquad (2)$$

Accordingly, the total axial stresses can be calculated by adding the thermal axial stresses and the dragdown stresses to the mechanical axial stresses $\sigma_{aMechanical}$ due to the building load that are constant with time which were reported by Murphy and McCartney (2015), as follows:

$$\sigma_{aTotal} = \sigma_{aT} + \sigma_{aD} + \sigma_{aMechanical} \qquad (3)$$

The thermal axial stresses, dragdown axial stresses, mechanical axial stresses, and total axial stresses for the last observed cases of extreme heating and cooling are shown in Figures 9(a) and 9(b) for Energy Piles A and B, respectively. After correction for dragdown, the total axial stresses in the energy piles varied between 5158 and 12508 kPa for Energy Pile A and 1760 and 10791 kPa for Energy Pile B. Although these values are higher than the maximum compressive stress permitted in drilled shafts with a compressive strength f'c of 21000 kPa (e.g., the International Building Code limits the axial stresses to 0.3f'c), the drilled shafts under this building were not designed a-priori to be energy piles. The analysis presented in this study is simplified, but emphasizes that the process to calculate the long-term axial stresses in energy piles depends on whether the axial strains occur due to thermo-elastic effects of the reinforced concrete, thermal effects on the subsurface, or long-term external loading effects.

Although it is assumed that the thermo-elastic expansion and contraction of the energy pile is isolated from the temporal dragdown/uplift process, this may not always be the case. This analysis assumes that the temporal dragdown/uplift process applies gradually greater axial stresses to the pile, but does not lead to sufficient displacements that the thermo-mechanical response of the energy pile would lead to plastic softening or ratcheting behavior. For example, if the energy piles were loaded very close to their ultimate capacity, the shape of the side shear stress-displacement curves may be such that the additional downward strains due to the dragdown process would lead to a more nonlinear response during heating and cooling. This was likely not the case in the energy piles evaluated here as they appeared to remain thermo-elastic during heating and cooling, but should be considered in other energy piles installed in soil profiles that could experience dragdown or uplift.

Conclusions

This study involved a comparison of thermal axial strain profiles measured in two energy piles at different moments of extreme heating and cooling over a five year period. The comparison indicates that a temporal dragdown/uplift process is superimposed atop the thermo-mechanical response of the energy pile. The dragdown strains estimated from comparison of the thermal axial strains at extreme heating were found to lead to a logical correction of thermal axial strains at extreme cooling. The mobilized coefficients of thermal expansion of the energy piles (i.e., the slope of temperature versus strain) were not observed to change significantly after several heating and cooling cycles, which indicates that the temporal downdrag/uplift is independent from the thermal expansion and contraction of the energy piles due to heating and cooling, respectively. The isolation of the dragdown/uplift effect from the thermo-elastic expansion and contraction of the energy piles permitted a more rational interpretation of the ranges in axial stress encountered during heating and cooling of the energy piles.

Acknowledgements

The authors acknowledge the support of Milender-White Construction Company, KL&A Structural Engineers, AMI Mechanical, Rocky Mountain Geothermal, and the Denver Housing Authority for agreeing to incorporate the energy piles and instrumentation into the building and to periodically access the site. Financial support from National Science Foundation grant CMMI 0928159 is appreciated.

References

Abdelaziz SL, Ozudogru TY. Non uniform thermal strains and stresses in energy piles. *Environmental Geotechnics*. 2016. DOI: 10.1680/jenge.15.00032.

Amatya BL, Soga K, Bourne-Webb PJ, Amis T, Laloui L Thermo-mechanical behaviour of energy piles. *Géotechnique*. 2012; 62(6): 503–519

Akrouch G, Sánchez M, Briaud J-L. Thermo-mechanical behavior of energy piles in high plasticity clays. *Acta Geotechnica*. 2014; 9(3): 399-412.

Asakawa, M. Reduction of skin friction between soil and metal wall by the electro-osmosis method. *Trans. of Japan Soc. of Civil Engineers*. 1959; 64, 55-65.

Bourne-Webb PJ, Amatya B, Soga K, Amis T, Davidson C, Payne P. Energy pile test at Lambeth College, London: Geotechnical and thermodynamic aspects of pile response to heat cycles. *Géotechnique*. 2009; 59(3): 237–248.

Bjerrum L, Johannessen IJ, Eide O. Reduction of negative skin friction on steel piles to rock. *Proc.*, *7th Int. Conf. on Soil Mech. and Found. Eng*. Sociedad Mexicana de Mecanica, Mexico City. 1969; 2, 27-34.

Brandl H. Energy foundations and other thermo-active ground structures. *Géotechnique*. 2006; 56(2): 81-122.

Budge AS, Dasenbrock DD, Mattison DJ. A synthesis of pile performance monitoring projects in downdrag environments in Minnesota. *IFCEE 2015*. 2015; 457-471.

Caulk R, Ghazanfari E, McCartney JS. Parameterization of a calibrated geothermal energy pile model. *Geomechanics for Energy and the Environment*. 2016; 5(3): 1-15. 10.1016/j.gete.2015.11.001.

Di Donna, A., Rotta Loria, A. and Laloui, L. Numerical study of the response of a group of energy piles under different combinations of thermo-mechanical loads. *Computers and Geotechnics*. 2015; 72(February): 126–142.

Fellenius BH. Downdrag on piles in clay due to negative skin friction. *Canadian Geotechnical Journal*. 1972; 9(4): 323-337.

Goode JC III, McCartney JS. Centrifuge modeling of end-restraint effects in energy foundations. *Journal of Geotechnical and Geoenvironmental Engineering*. 2015; 141(8): 04015034-1-13.

Laloui L, Nuth M, Vulliet L. Experimental and numerical investigations of the behaviour of a heat exchanger pile. *International Journal of Numerical and Analytical Methods in Geomechanics*. 2006; 30(8): 763–781.

Laloui L, Olgun CG, Sutman M, McCartney JS, Coccia CJR, Abuel-Naga HM, Bowers GA. Issues involved with thermo-active geotechnical systems: Characterization of thermo-mechanical soil behavior and soil-structure interface behavior. *The Journal of the Deep Foundations Institute*. 2014; 8(2): 107-119.

McCartney JS, Murphy KD. Strain distributions in full-scale energy foundations. *DFI Journal*. 2012; 6(2): 28-36.

Murphy KD, McCartney JS. Seasonal response of energy foundations during building operation. *Geotechnical and Geological Engineering*. 2015; 33(2): 343-356.

Murphy KD, McCartney JS, Henry KS. Thermo-mechanical response tests on energy foundations with different heat exchanger configurations. *Acta Geotechnica*. 2015; 10(2): 179-195.

Olgun CG, McCartney JS. Outcomes from the International Workshop on Thermoactive Geotechnical Systems for Near-Surface Geothermal Energy: From research to practice. *The Journal of the Deep Foundations Institute*. 2014; 8(2): 58-72.

Pasten C, Santamarina JC. Thermally induced long-term displacement of thermoactive piles. *Journal of Geotechnical and Geoenvironmental Engineering*. 2014; 140(5): 06014003.

Saggu R, Chakraborty T. Cyclic thermo-mechanical analysis of energy piles in sand. *Geotechnical and Geological Engineering*. 2015; 33(3): 321-342.

Suryatriyastuti ME, Mroueh H, Burlon S. A load transfer approach for studying the cyclic behavior of thermo-active piles. *Computers and Geotechnics*. 2014; 55: 378–391.

Wang B, Bouazza A, Singh R, Haberfield C, Barry-Macaulay D, Baycan S. Post-temperature effects on shaft capacity of a full-scale geothermal energy pile." *Journal of Geotechnical and Geoenvironmental Engineering*. 2014; 04014125. 10.1061/(ASCE)GT.1943-5606.0001266.

List of Figure Captions

Fig. 1. Schematics of the energy piles including locations of instrumentation

FIG. 2. Heat exchanger fluid temperatures: (a) Energy Pile A; (b) Energy Pile B

FIG. 3. Energy pile time series: (a) Temperature fluctuations in Energy Pile A; (b) Temperature fluctuations in Energy Pile B; (c) Change in temperature in Energy Pile A; (d) Change in temperature in Energy Pile B; (e) Thermal axial strains in Energy Pile A; (f) Thermal axial strains in Energy Pile B

FIG. 4. Comparison between average pile temperature and outlet fluid temperature: (a) Energy Pile A; (b) Energy Pile B

FIG. 5. Thermal expansion after different seasonal heating and cooling periods: (a) Transient thermal axial strain with change in temperature for Energy Pile A; (b) Transient thermal axial strain with change in temperature for Energy Pile B; (c) Distribution of average mobilized coefficients of thermal expansion for Energy Pile A; (d) Distribution of average mobilized coefficients of thermal expansion for Energy Pile B

FIG. 6. Moments in time with similar average changes in pile temperature in Energy Pile A: (a) Temperatures during extreme heating; (b) Temperature during extreme cooling; (c) Thermal axial strains during extreme heating; (d) Thermal axial strains during extreme cooling

FIG. 7. Moments in time with similar average changes in pile temperature in Energy Pile B: (a) Temperatures during extreme heating; (b) Temperature during extreme cooling; (c) Thermal axial strains during extreme heating; (d) Thermal axial strains during extreme cooling

FIG. 8. Dragdown/uplift effect evaluation: (a) Extreme heating in Energy Pile A; (b) Extreme heating in Energy Pile B; (c) Extreme cooling in Energy Pile A; (d) Extreme cooling in Energy Pile B

FIG. 9. Axial stress evaluation; (a) Energy Pile A; (b) Energy Pile B

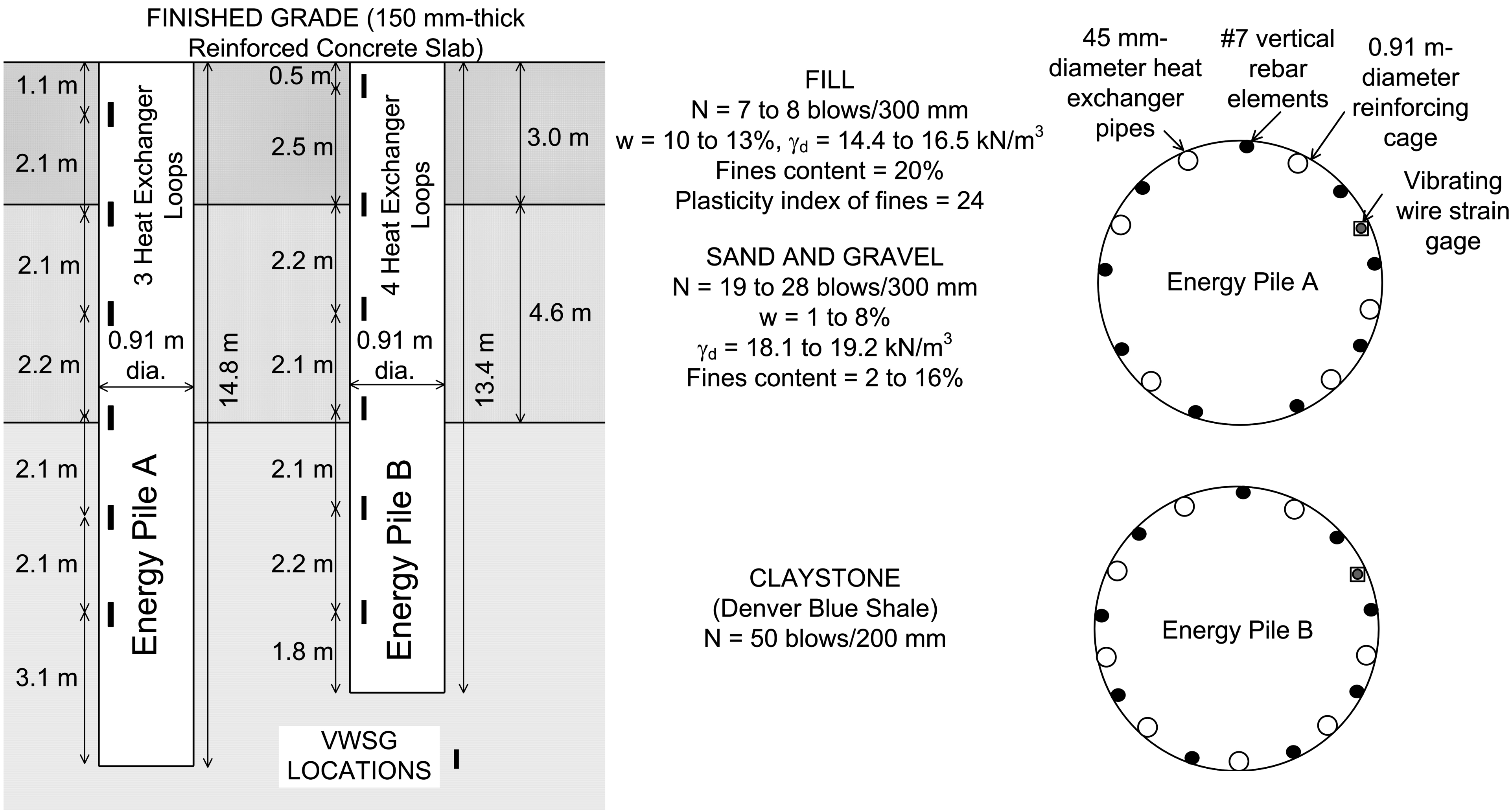

FINISHED GRADE (150 mm-thick Reinforced Concrete Slab)
1.1 m
2.1 m
2.1 m
2.2 m
2.1 m
2.1 m
3.1 m
3 Heat Exchanger Loops
0.91 m dia.
Energy Pile A
14.8 m
0.5 m
2.5 m
2.2 m
2.1 m
2.1 m
2.2 m
1.8 m
4 Heat Exchanger Loops
0.91 m dia.
Energy Pile B
13.4 m
3.0 m
4.6 m
VWSG LOCATIONS
FILL
N = 7 to 8 blows/300 mm
w = 10 to 13%, γ_d = 14.4 to 16.5 kN/m^3
Fines content = 20%
Plasticity index of fines = 24
SAND AND GRAVEL
N = 19 to 28 blows/300 mm
w = 1 to 8%
γ_d = 18.1 to 19.2 kN/m^3
Fines content = 2 to 16%
CLAYSTONE
(Denver Blue Shale)
N = 50 blows/200 mm
45 mm-diameter heat exchanger pipes
#7 vertical rebar elements
0.91 m-diameter reinforcing cage
Vibrating wire strain gage
Energy Pile A
Energy Pile B

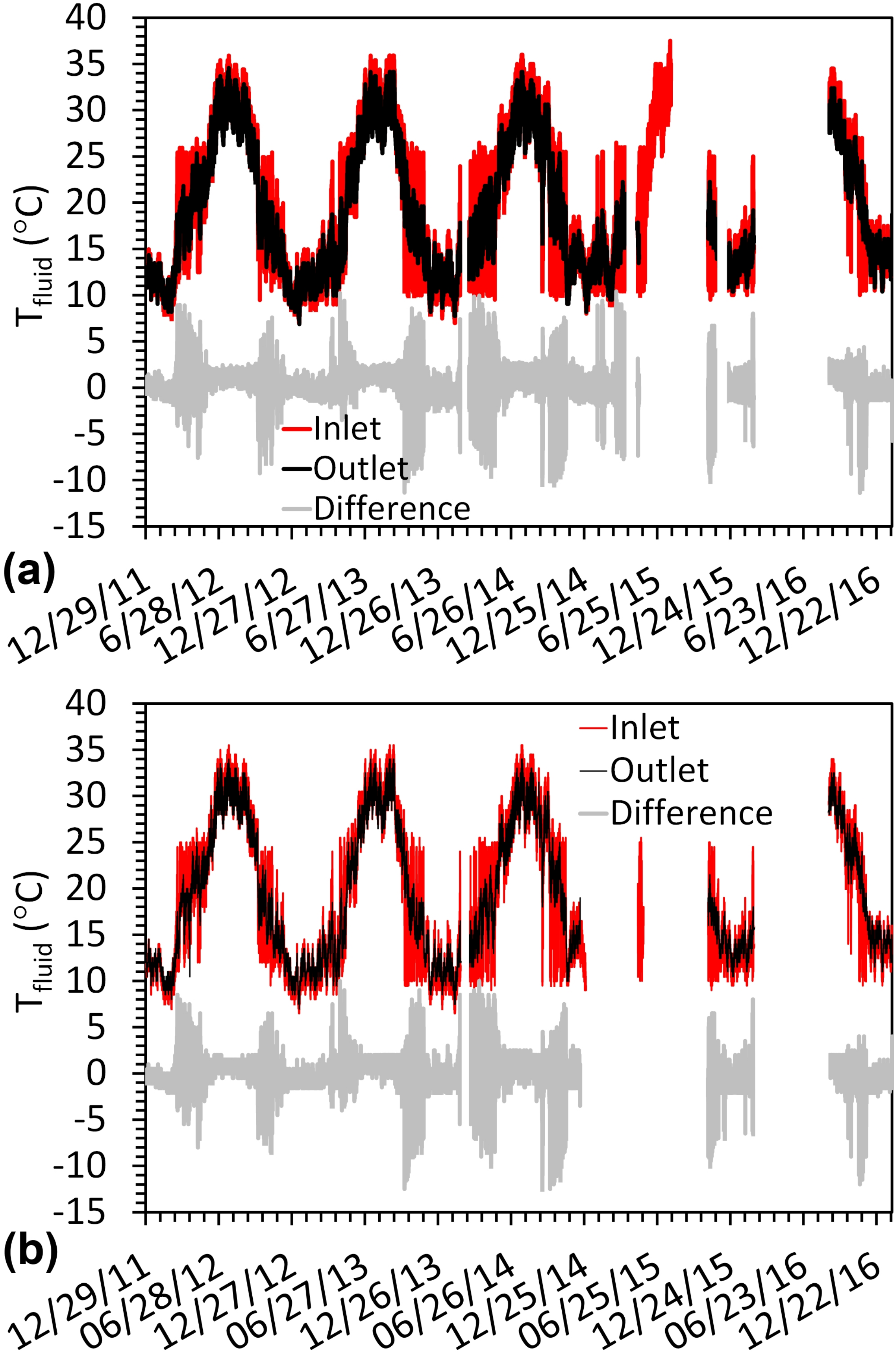

(a)
T_fluid (°C)
40
35
30
25
20
15
10
5
0
-5
-10
-15
Inlet
Outlet
Difference
12/29/11
6/28/12
12/27/12
6/27/13
12/26/13
6/26/14
12/25/14
6/25/15
12/24/15
6/23/16
12/22/16
(b)
T_fluid (°C)
40
35
30
25
20
15
10
5
0
-5
-10
-15
Inlet
Outlet
Difference
12/29/11
06/28/12
12/27/12
06/27/13
12/26/13
06/26/14
12/25/14
06/25/15
12/24/15
06/23/16
12/22/16

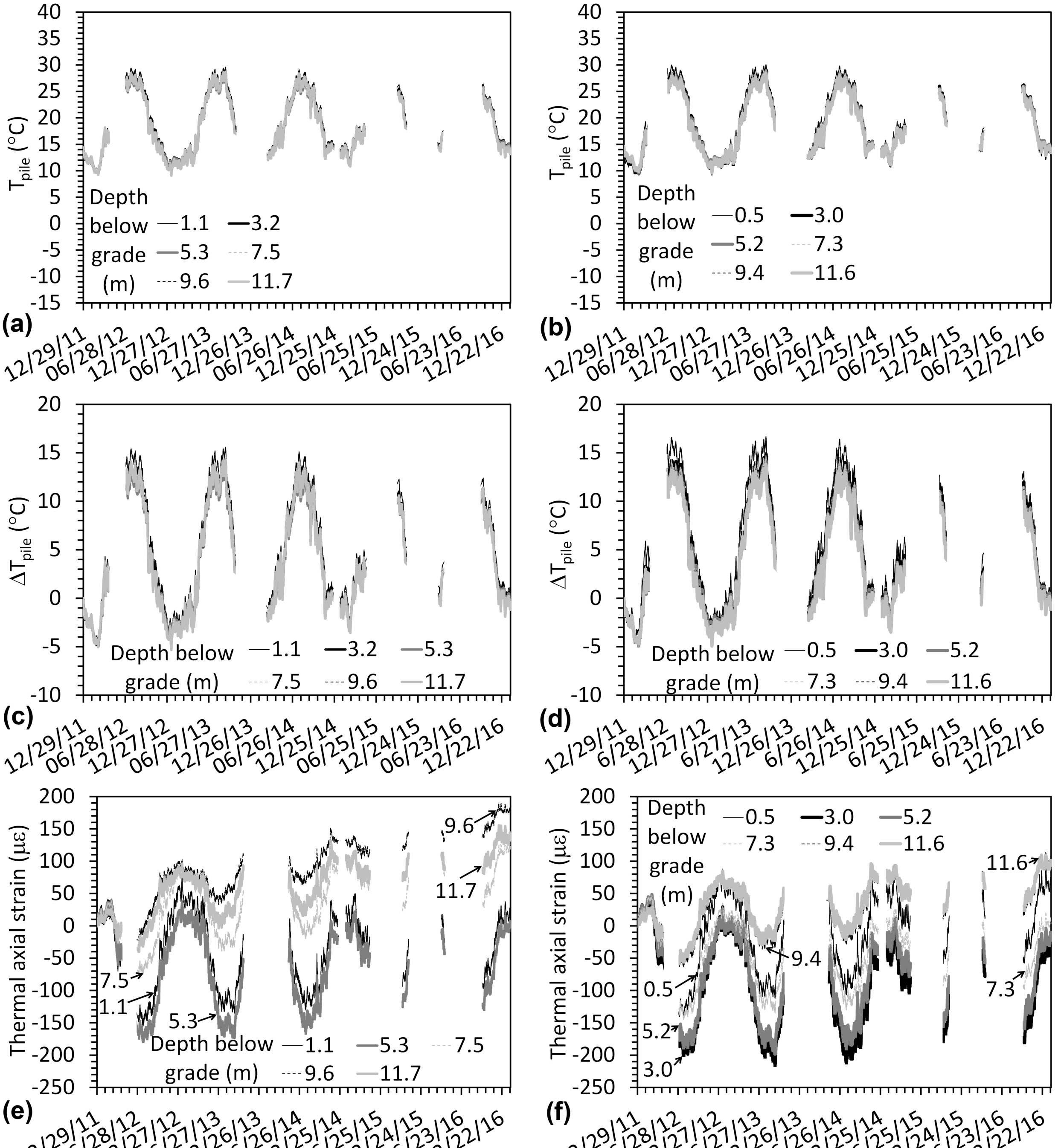

(a)
(b)
(c)
(d)
(e)
(f)
T_{pile} (°C)
ΔT_{pile} (°C)
Thermal axial strain (με)
Depth below grade (m)
1.1
3.2
5.3
7.5
9.6
11.7
0.5
3.0
5.2
7.3
9.4
11.6
12/29/11
06/28/12
12/27/12
06/27/13
12/26/13
06/26/14
12/25/14
06/25/15
12/24/15
06/23/16
12/22/16

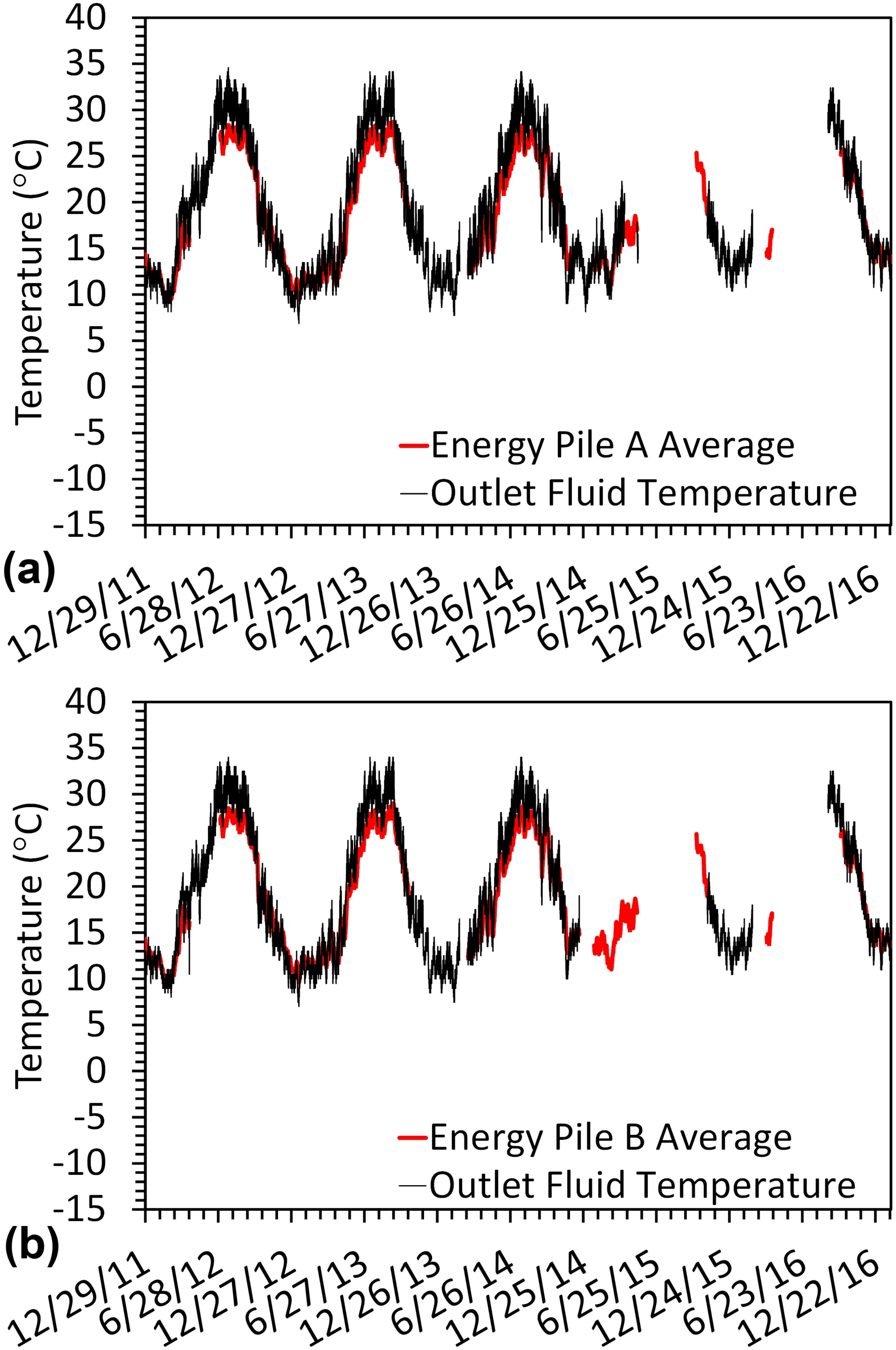
(a)
Temperature (°C)
40
35
30
25
20
15
10
5
0
-5
-10
-15
Energy Pile A Average
Outlet Fluid Temperature
12/29/11
6/28/12
12/27/12
6/27/13
12/26/13
6/26/14
12/25/14
6/25/15
12/24/15
6/23/16
12/22/16
(b)
Temperature (°C)
Energy Pile B Average
Outlet Fluid Temperature

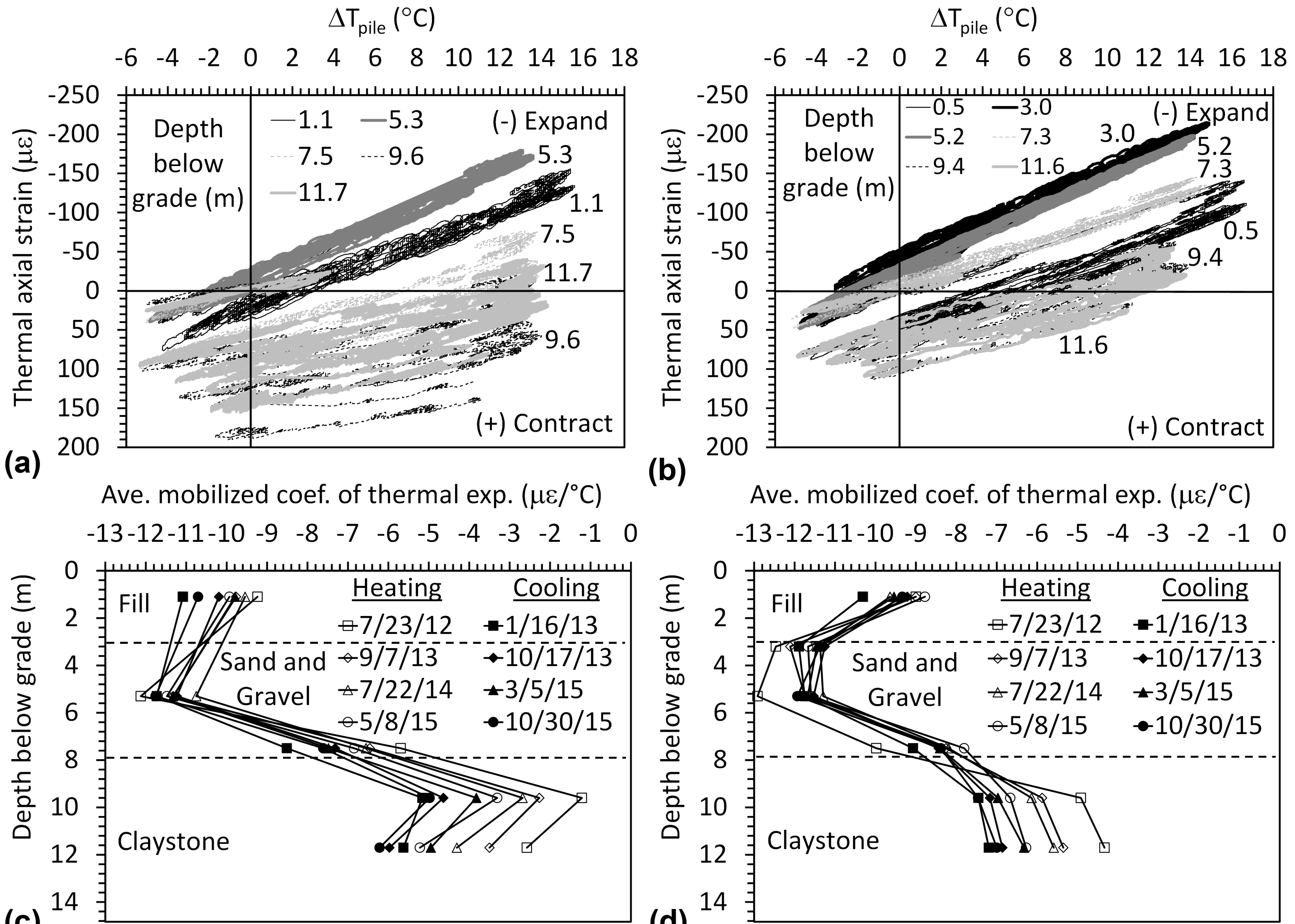

ΔT_pile (°C)
Thermal axial strain (με)
Depth below grade (m)
(-) Expand
(+) Contract
1.1
5.3
7.5
9.6
11.7
(a)
0.5
3.0
5.2
7.3
9.4
11.6
(b)
Ave. mobilized coef. of thermal exp. (με/°C)
Depth below grade (m)
Fill
Sand and Gravel
Claystone
Heating
Cooling
7/23/12
1/16/13
9/7/13
10/17/13
7/22/14
3/5/15
5/8/15
10/30/15
(c)
(d)

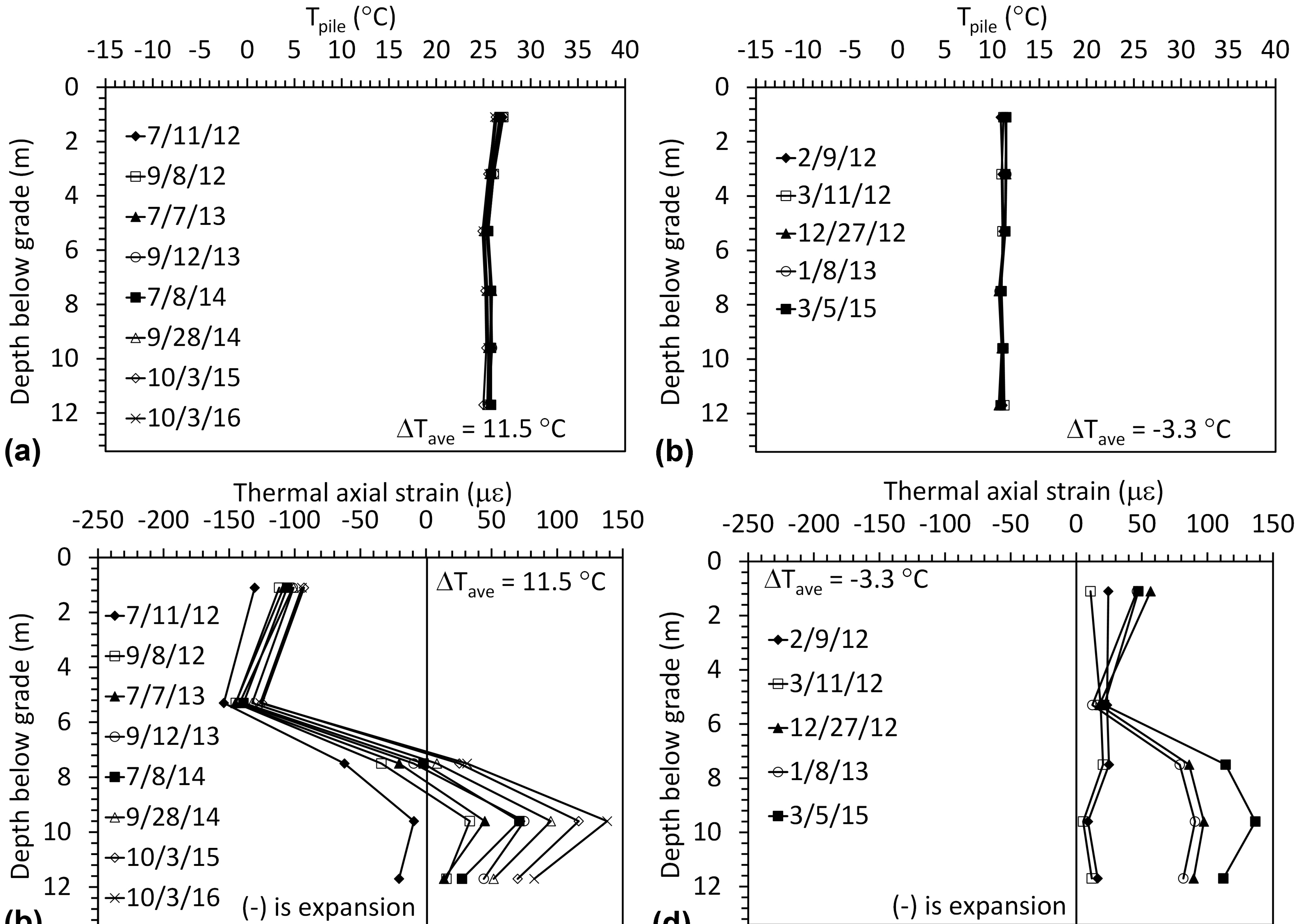

T_pile (°C)
-15 -10 -5 0 5 10 15 20 25 30 35 40
Depth below grade (m)
0 2 4 6 8 10 12
7/11/12
9/8/12
7/7/13
9/12/13
7/8/14
9/28/14
10/3/15
10/3/16
ΔT_ave = 11.5 °C
(a)
T_pile (°C)
2/9/12
3/11/12
12/27/12
1/8/13
3/5/15
ΔT_ave = -3.3 °C
(b)
Thermal axial strain (με)
-250 -200 -150 -100 -50 0 50 100 150
ΔT_ave = 11.5 °C
(-) is expansion
(b)
Thermal axial strain (με)
ΔT_ave = -3.3 °C
(-) is expansion
(d)

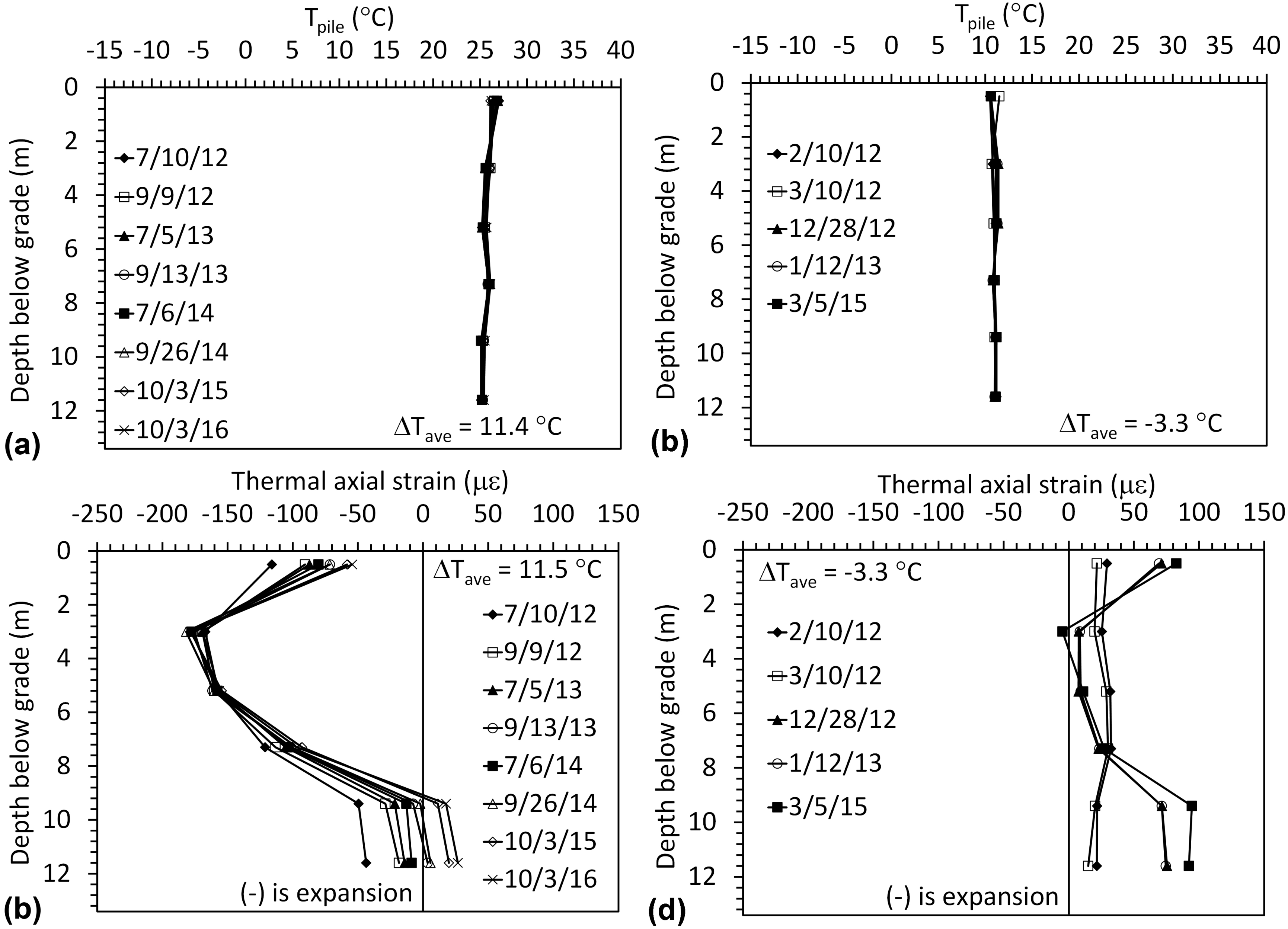

T_{pile} (°C)
-15 -10 -5 0 5 10 15 20 25 30 35 40
Depth below grade (m)
0 2 4 6 8 10 12
7/10/12
9/9/12
7/5/13
9/13/13
7/6/14
9/26/14
10/3/15
10/3/16
ΔT_{ave} = 11.4 °C
(a)
T_{pile} (°C)
2/10/12
3/10/12
12/28/12
1/12/13
3/5/15
ΔT_{ave} = -3.3 °C
(b)
Thermal axial strain (με)
-250 -200 -150 -100 -50 0 50 100 150
ΔT_{ave} = 11.5 °C
(-) is expansion
(b)
Thermal axial strain (με)
ΔT_{ave} = -3.3 °C
(-) is expansion
(d)

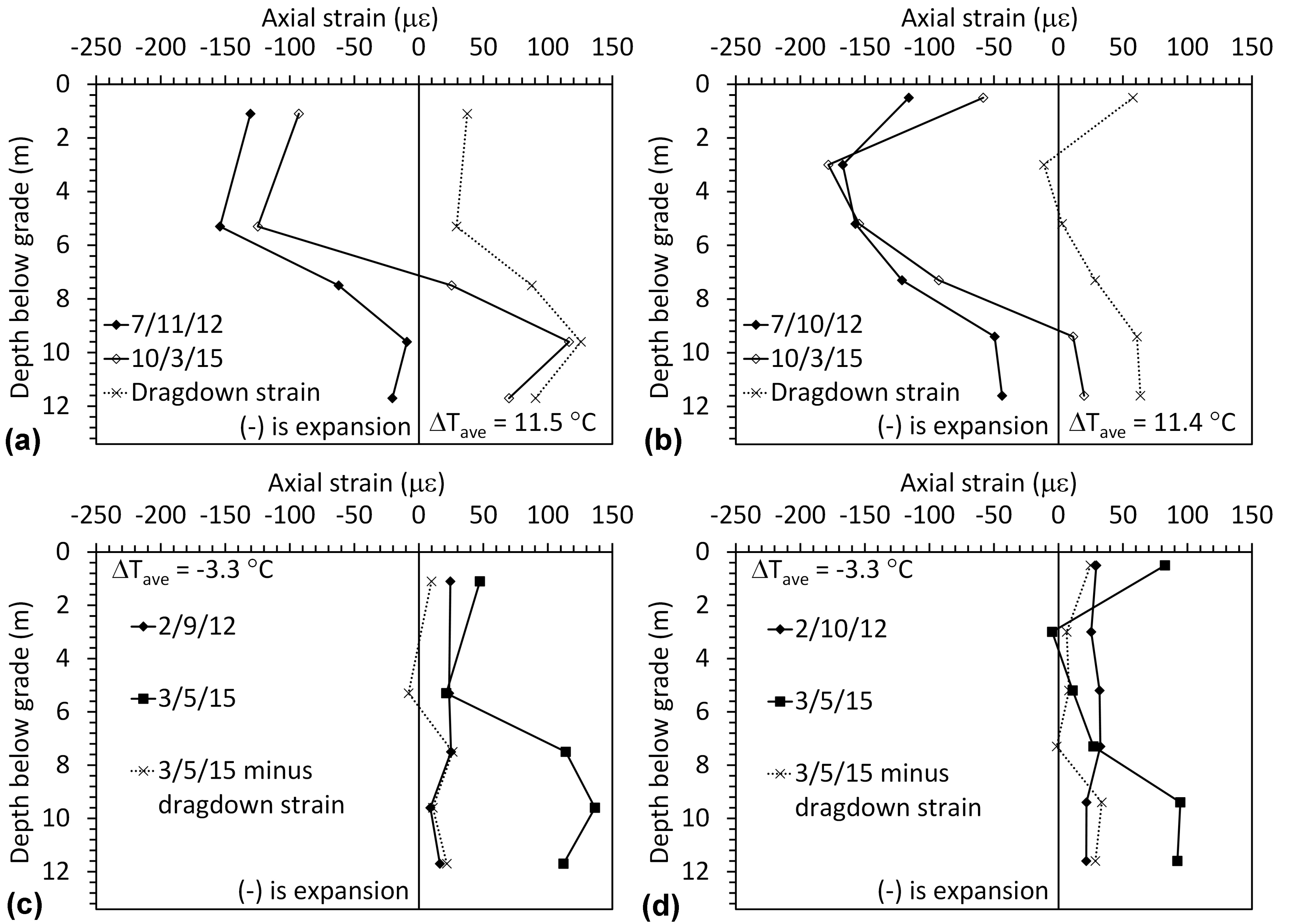

Axial strain (με)
-250 -200 -150 -100 -50 0 50 100 150
Depth below grade (m)
0 2 4 6 8 10 12
7/11/12
10/3/15
Dragdown strain
(-) is expansion
ΔT_ave = 11.5 °C
(a)
7/10/12
10/3/15
Dragdown strain
(-) is expansion
ΔT_ave = 11.4 °C
(b)
ΔT_ave = -3.3 °C
2/9/12
3/5/15
3/5/15 minus dragdown strain
(-) is expansion
(c)
ΔT_ave = -3.3 °C
2/10/12
3/5/15
3/5/15 minus dragdown strain
(-) is expansion
(d)

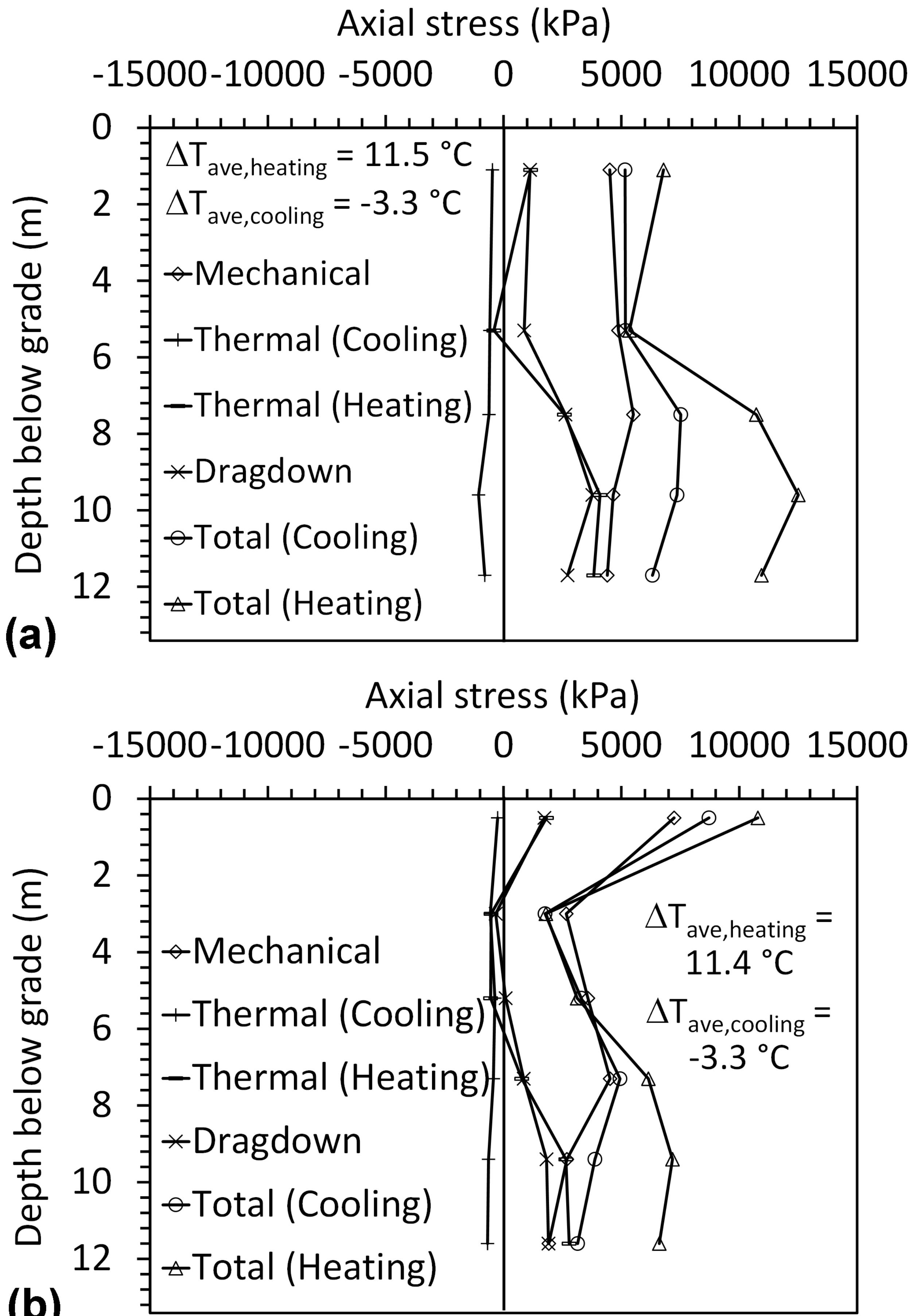

Axial stress (kPa)
-15000 -10000 -5000 0 5000 10000 15000
Depth below grade (m)
0 2 4 6 8 10 12
ΔT_ave,heating = 11.5 °C
ΔT_ave,cooling = -3.3 °C
Mechanical
Thermal (Cooling)
Thermal (Heating)
Dragdown
Total (Cooling)
Total (Heating)
(a)
Axial stress (kPa)
-15000 -10000 -5000 0 5000 10000 15000
Depth below grade (m)
0 2 4 6 8 10 12
ΔT_ave,heating = 11.4 °C
ΔT_ave,cooling = -3.3 °C
Mechanical
Thermal (Cooling)
Thermal (Heating)
Dragdown
Total (Cooling)
Total (Heating)
(b)

Highlights:

The paper is focused on a reinterpretation of axial strain data from a pair of energy piles that have undergone heating and cooling as part of a building heat pump operation over the course of four and a half years. It was concluded that a temporal dragdown effect has been superimposed atop the thermal axial strain measurements. A simple interpretation presented in the paper permits isolation of the thermal and dragdown effects on the axial strain, which further permits evaluation of the axial stresses in the pile during heating and cooling.